Supplementary Materials

Au-Fe Separates Enable CO-Assisted Methane Oxidation to Acetic Acid with O_2 via Tandem Catalysis

Hongfei Lin [1], Haibin Yin [1,*], Chuyue Meng [1], Chengyuan Liu [2], Long Zhao [2], Hongliang Li [1], Bo Wu [1,3,*], and Jie Zeng [1,4,5,*]

[1] Hefei National Research Center for Physical Sciences at the Microscale, CAS Key Laboratory of Strongly-Coupled Quantum Matter Physics, Key Laboratory of Surface and Interface Chemistry and Energy Catalysis of Anhui Higher Education Institutes, Department of Chemical Physics, University of Science and Technology of China, Hefei 230026, China
[2] National Synchrotron Radiation Laboratory, University of Science and Technology of China, Hefei, 230026, China
[3] Oxide & Organic Nanomaterials for Energy & Environment Laboratory, Chemistry Program, Physical Science & Engineering, King Abdullah University of Science and Technology, Thuwal 23955, Saudi Arabia
[4] School of Chemistry & Chemical Engineering, Anhui University of Technology, Ma'anshan 243002, China
[5] Deep Space Exploration Laboratory, Hefei 230088, China
* Correspondence: yinhb@ustc.edu.cn (H.Y.); bo.wu@kaust.edu.sa (B.W.); zengj@ustc.edu.cn (J.Z.)
Received: 9 June 2026; Revised: 23 June 2026; Accepted: 28 June 2026; Published: 30 June 2026

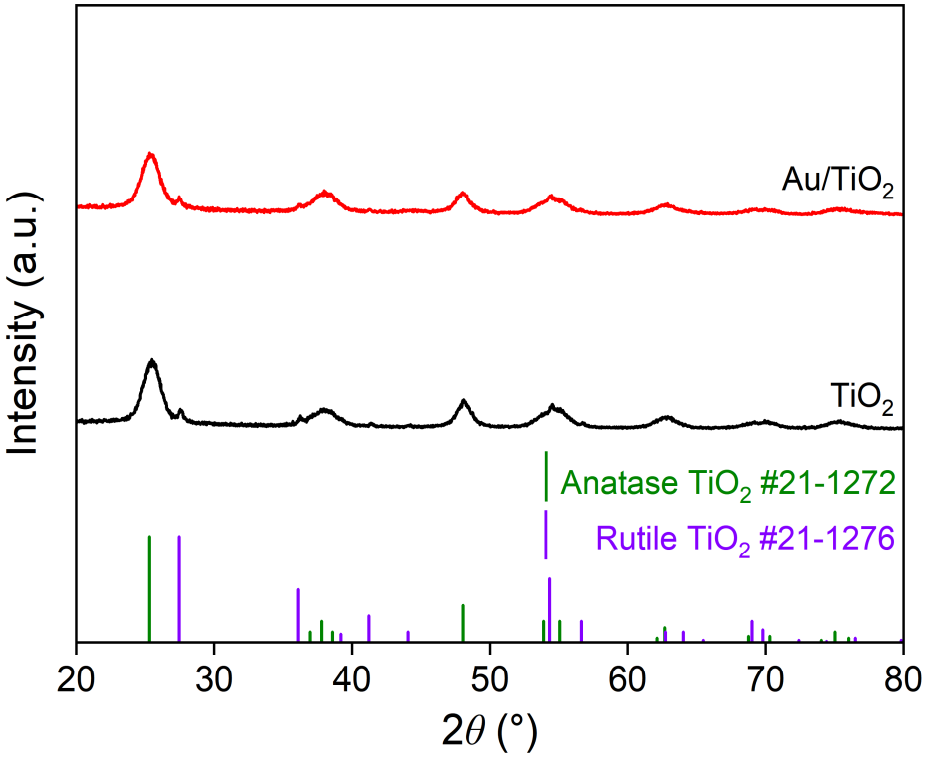

Figure S1. XRD patterns of TiO_2 and Au/TiO_2.

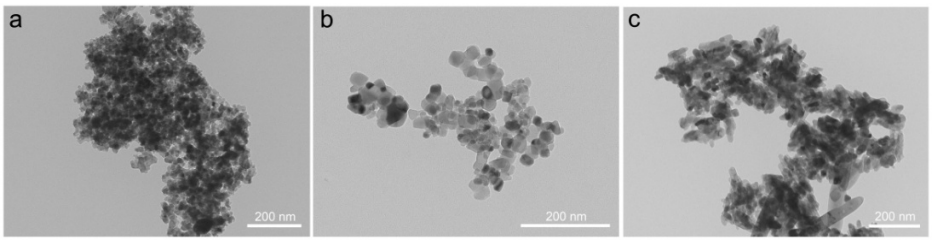

Figure S2. TEM images for TiO_2 supported Au-based catalysts. (**a**) Au/TiO_2-A. (**b**) Au/TiO_2-P25. (**c**) Au/TiO_2-R.

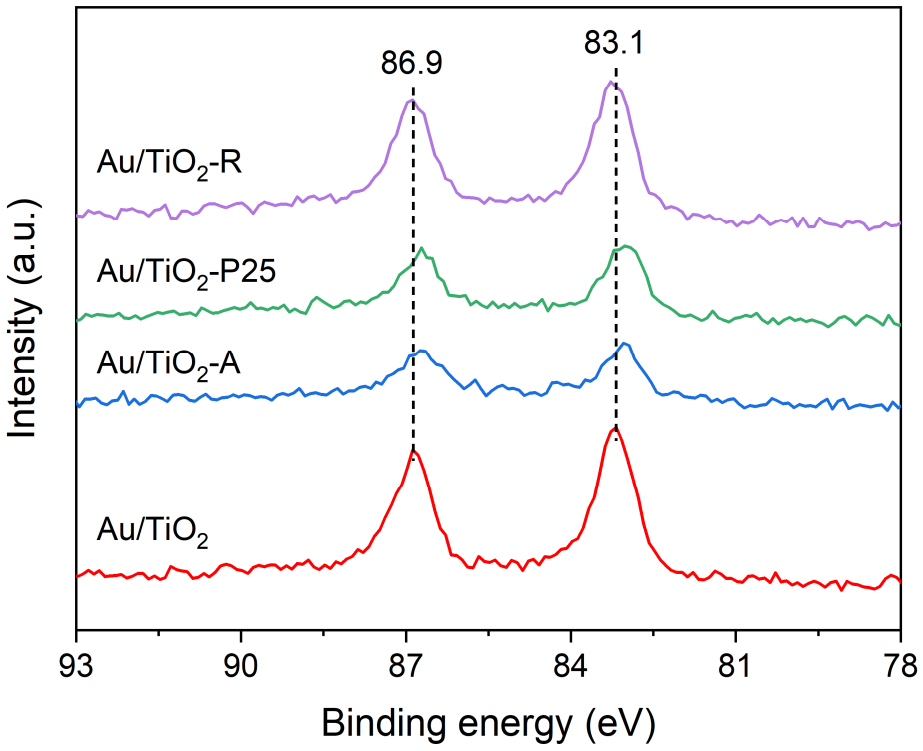

Figure S3. Au 4*f* XPS spectra of Au/TiO_2, Au/TiO_2-A, Au/TiO_2-P25, and Au/TiO_2-R.

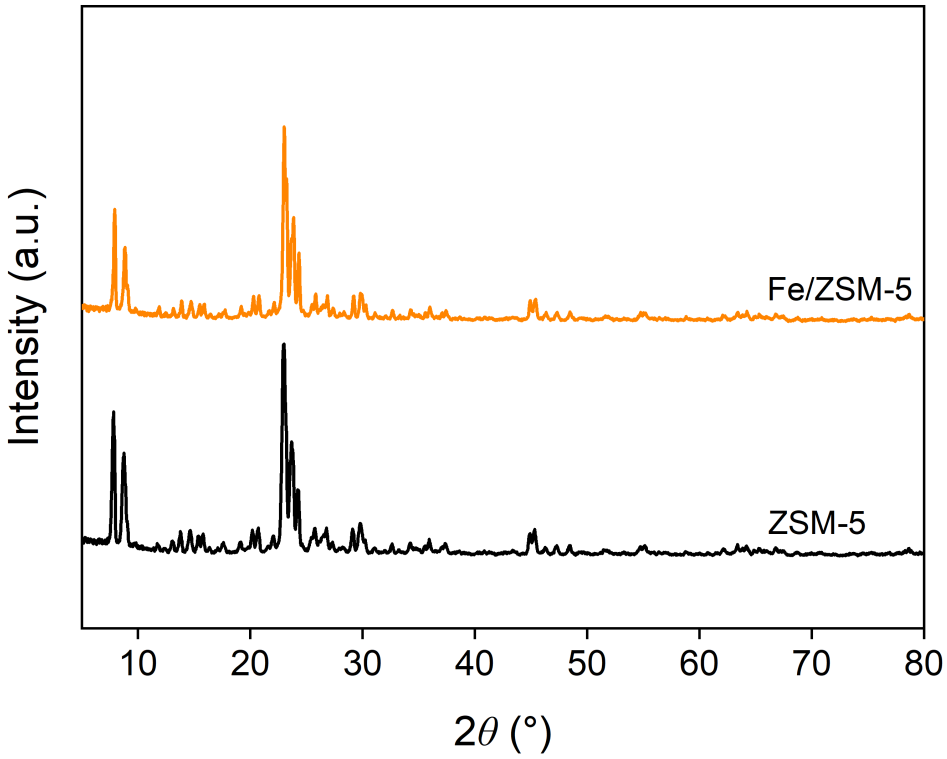

Figure S4. XRD patterns of ZSM-5 and Fe/ZSM-5.

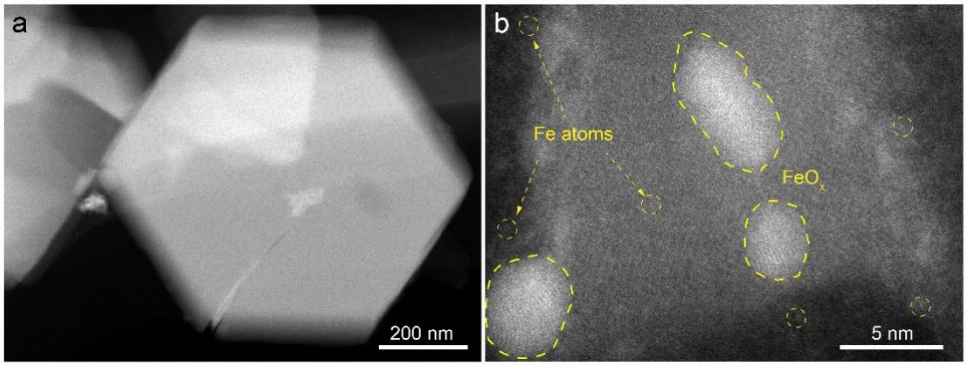

Figure S5. HAADF-STEM characterizations of Fe/ZSM-5-imp. (**a**) and (**b**) HAADF-STEM images of Fe/ZSM-5-imp.

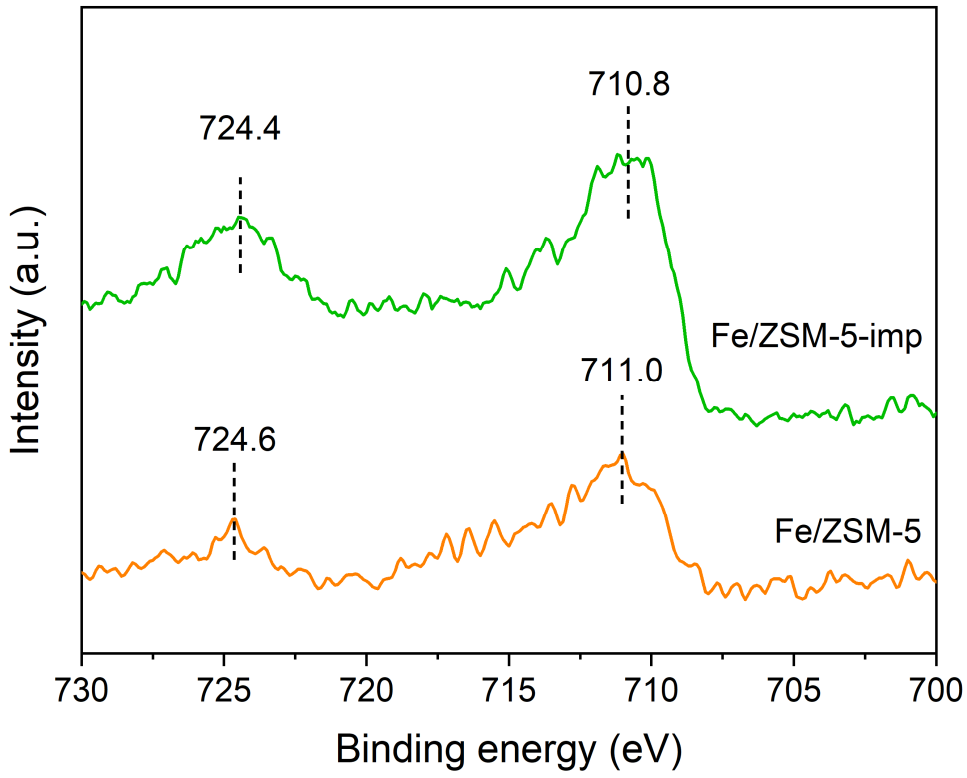

Figure S6. Fe 2*p* XPS spectra of Fe/ZSM-5 and Fe/ZSM-5-imp.

Table S1. ICP-AES results of all the samples.

Entry	Catalyst	Metal Loading (wt%)	
		Au	Fe
1	Au/TiO_2	1.7	/
2	Au/TiO_2-A	1.6	/
3	Au/TiO_2-P25	1.7	/
4	Au/TiO_2-R	1.6	/
5	Fe/ZSM-5	/	1.0
6	Fe/ZSM-5-imp	/	1.0

Table S2. The deconvolution result of UV-Vis spectra of ZSM-5, Fe/ZSM-5, and Fe/ZSM-5-imp.

Catalyst	Percentage of Fe species (%)			
	MT Fe^{3+}	MO Fe^{3+}	Fe_xO_y	Fe_2O_3
ZSM-5	64.6	35.4	0	0
Fe/ZSM-5	49.8	12.9	22.5	14.8
Fe/ZSM-5-imp	29.5	11.8	17.5	41.2

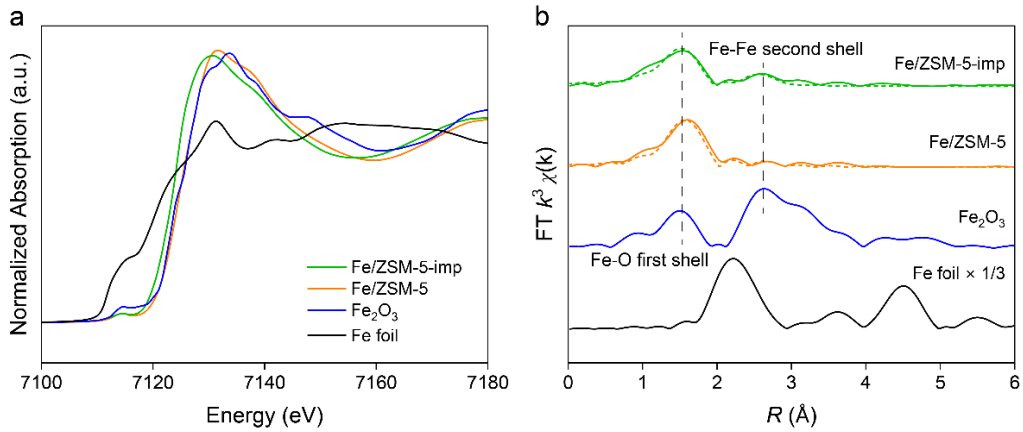

Figure S7. XAS measurements of Fe foil, Fe_2O_3, Fe/ZSM-5, and Fe/ZSM-5-imp. (**a**) Normalized Fe *K*-edge XANES spectra. (**b**) k^3-weighted Fe *K*-edge EXAFS spectra.

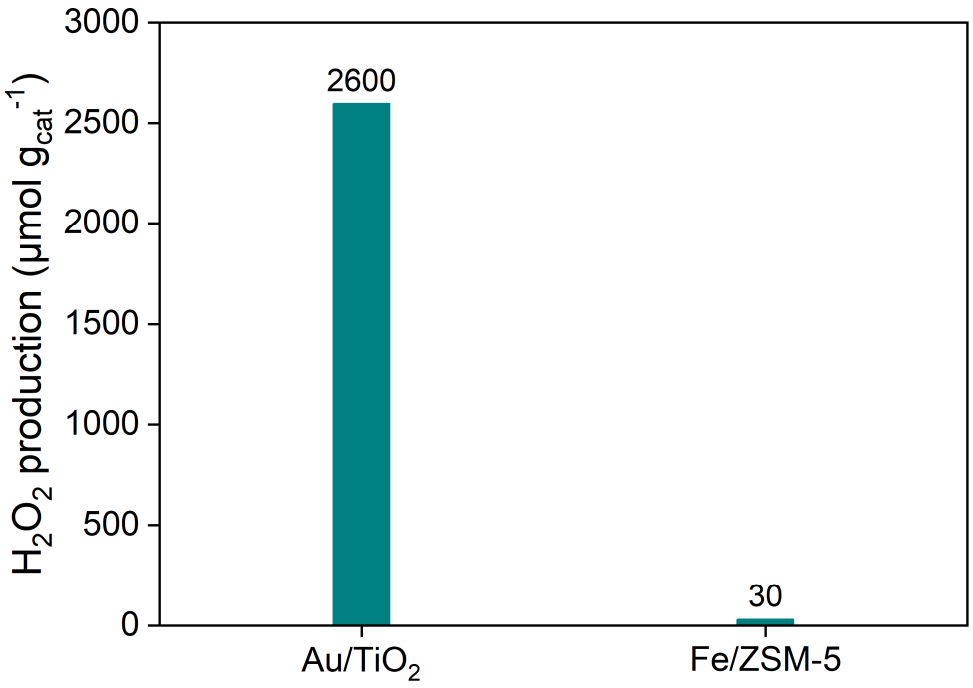

Figure S8. H_2O_2 synthesis over Au/TiO_2 and Fe/ZSM-5. The reaction was conducted over 15 mg of the catalyst with mechanical stirring (1000 rpm) in 15 mL of H_2O under 40 bar of CO, 6 bar of O_2, and 15 bar of N_2 at 30 °C for 1 h.

Table S3. EXAFS fitting results of Fe foil and Fe-containing samples. *CN* refers to the coordination number. *R* refers to the bond length. σ^2 refers to the Debye-Waller factor. ΔE_0 refers to the inner potential correction to account for the difference in the inner potential between the sample and the reference compound. *R*-factor refers to the goodness of fit.

Sample	Shell	*CN*	*R* (Å)	σ^2 (Å^2)	ΔE_0 (eV)	*R*-Factor
Fe foil	Fe-Fe	8	2.48	-	-	-
	Fe-Fe	6	2.86			
Fe/ZSM-5	Fe-O	5.3 ± 0.3	2.04 ± 0.01	0.007	1.7 ± 1.3	0.016
	Fe-Fe	0.4 ± 0.7	3.06 ± 0.13	0.010	1.7 ± 1.3	
Fe/ZSM-5-imp	Fe-O	5.7 ± 0.8	2.01 ± 0.02	0.011	−0.6 ± 1.6	0.016
	Fe-Fe	1.7 ± 0.6	3.03 ± 0.06	0.010	1.3 ± 6.9	

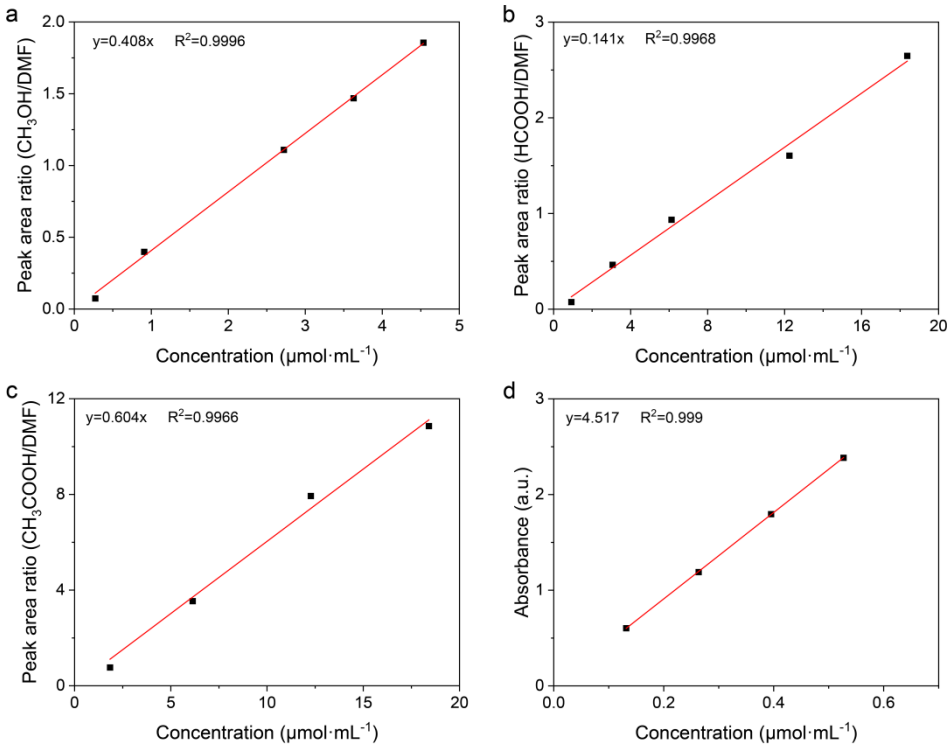

Figure S9. Standard calibration curves for oxygenates quantification. (**a**) CH_3OH. (**b**) HCOOH. (**c**) CH_3COOH. (**d**) $HOCH_2OH$.

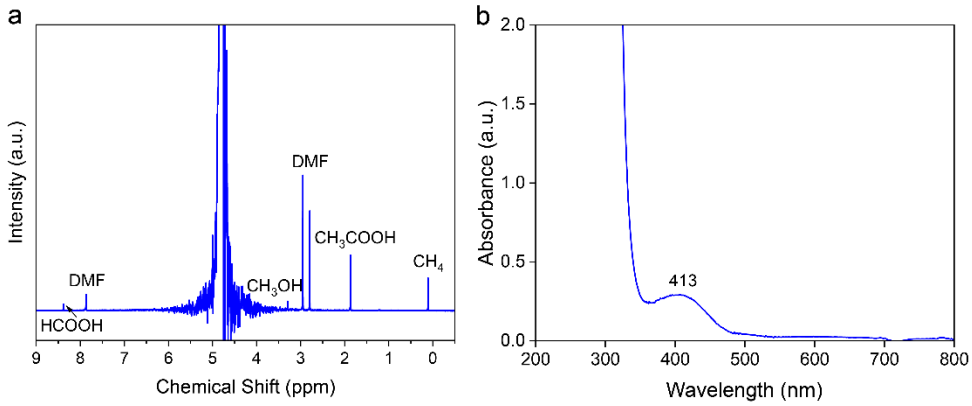

Figure S10. (**a**) and (**b**) Typical ^1H NMR and UV-Vis spectra.

Table S4. Adjusting the mass loading of Fe/ZSM-5 (0~100 mg) while maintaining a fixed Au/TiO_2 (15 mg) on methane oxidation. The reaction was conducted over Au/TiO_2 + Fe/ZSM-5 with mechanical stirring (1000 rpm) in 15 mL of H_2O under 15 bar of CH_4, 40 bar of CO, and 6 bar of O_2 at 30 °C for 6 h.

Mass of Fe/ZSM-5 (mg)	Products (μmol g_{cat}^{-1})					CH_3COOH Selectivity (%)
	CH_3COOH	HCOOH	$HOCH_2OH$	CH_3OH	Total	
0	0	0	0	0	0	0
15	55.6	0	14.1	19.9	89.6	62.1
30	58.2	21.2	11.1	19.9	110.4	52.7
60	60.3	25.5	11.5	19.9	117.2	51.5
100	66.3	24.9	9.7	7.8	108.7	61.0

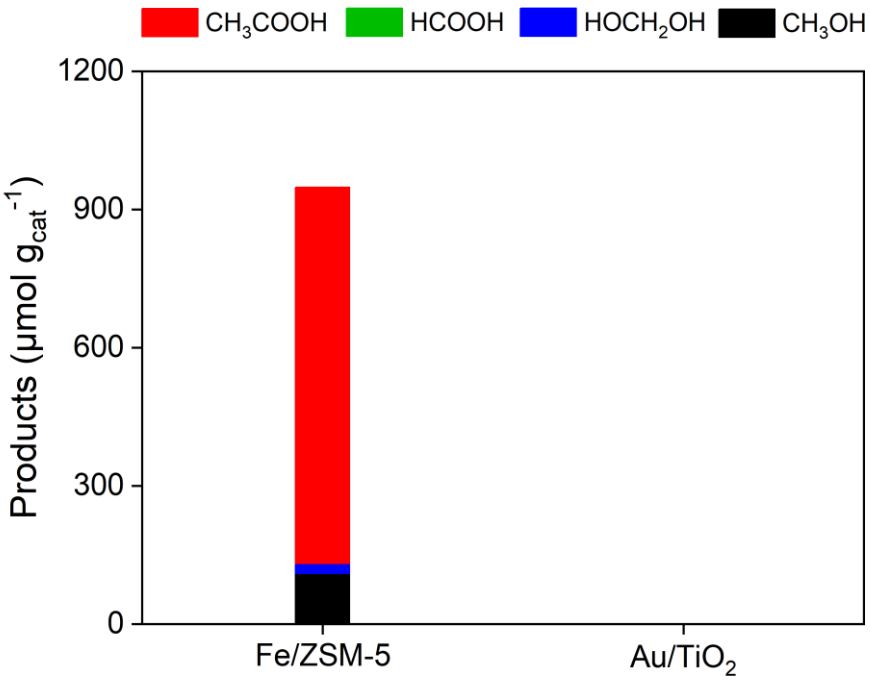

Figure S11. Methane oxidation with H_2O_2 in the presence of CO over Au/TiO_2 and Fe/ZSM-5. The reaction was conducted over 50 mg of the catalyst with mechanical stirring (1000 rpm) in 15 mL of H_2O containing 1500 μmol of H_2O_2 under 15 bar of CH_4, 40 bar of CO, and 6 bar of N_2 at 30 °C for 1 h.

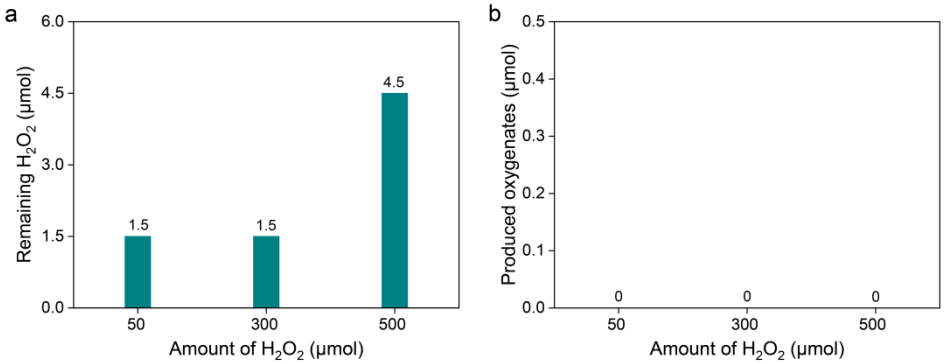

Figure S12. Methane oxidation with H_2O_2 as the oxidant over Au/TiO_2. (**a**) Remaining H_2O_2 after reaction. (**b**) Amount of produced oxygenates. The reaction was conducted over 50 mg of Au/TiO_2 with mechanical stirring (1000 rpm) in 15 mL of H_2O containing 50~500 μmol of H_2O_2 under 15 bar of CH_4 and 46 bar of N_2 at 30 °C for 1 h.

Table S5. Adjusting the mass loading of Au/TiO_2 (0~80 mg) while maintaining a fixed Fe/ZSM-5 (100 mg) on methane oxidation. The reaction was conducted over Au/TiO_2 + Fe/ZSM-5 with mechanical stirring (1000 rpm) in 15 mL of H_2O under 15 bar of CH_4, 40 bar of CO, and 6 bar of O_2 at 30 °C for 6 h.

Mass of Au/TiO_2 (mg)	**Products (μmol g_{cat}^{-1})**					**CH_3COOH Selectivity (%)**
	CH_3COOH	**HCOOH**	**$HOCH_2OH$**	**CH_3OH**	**Total**	
0	0	0	0	0	0	0
6	29.0	16.6	18.2	2.8	66.6	43.5
15	66.3	24.9	9.7	7.8	108.7	61.0
30	65.9	22.0	5.2	13.8	106.9	61.6
50	55.6	19.1	3.0	8.0	85.7	64.9
80	34.4	10.6	2.5	5.0	52.5	65.5

Table S6. Mass ratio effect of the Au/TiO_2 to Fe/ZSM-5 on methane oxidation. The reaction was conducted over a total catalyst mass of 150 mg with mechanical stirring (1000 rpm) in 15 mL of H_2O under 15 bar of CH_4, 40 bar of CO, and 6 bar of O_2 at 30 °C for 6 h.

Mass ratio of Au/TiO_2 to Fe/ZSM-5	Products (μmol g_{cat}^{-1})					CH_3COOH Selectivity (%)
	CH_3COOH	HCOOH	$HOCH_2OH$	CH_3OH	Total	
1/4	54.2	31.8	4.8	12.0	102.8	52.7
1/2	55.6	19.1	3.0	8.0	85.7	64.9
1/1	35.7	0	2.1	8.0	45.8	77.9
2/1	17.2	0	2.0	4.0	23.2	74.1
4/1	10.6	0	1.9	2.0	14.5	73.1

Table S7. Comparison of methane oxidation with O_2/H_2O_2 as the oxidants in the presence of CO at low temperatures.

Entry	Catalyst	Gas	T [°C]	CH_3COOH Yield [μmol g_{cat}^{-1} h^{-1}]	CH_3COOH in Liquid [%]	TOF_{Fe} [h^{-1}]	Reference
1	Au/TiO_2 + Fe/ZSM-5	CH_4 + CO + O_2	30	9.3	64.9	0.08	This work
			40	25.5	67.6	0.21	
			50	49.1	87.6	0.41	
			60	68.8	95.9	0.58	
2	Rh/ZSM-5	CH_4 + CO + O_2	25	0	0	/	[1]
			50	0	0	/	
3	Au-Fe/ZSM-5	CH_4 + CO + O_2	60	36.7	80.3	0.41	[2]
			80	366.7	85.0	4.11	
4	Rh/TiO_2 + $CuCl_2$	CH_4 + CO + O_2	100	0.0	0.0	/	[3]
5	Rh-Fe/MoS_2	CH_4 + CO + O_2	25	26.2	90.3	0.05	[4]
			80	105.6	95.6	0.18	
6	As-prepared Ir	CH_4 + CO + O_2	110	500.0	N.A.	/	[5]
7	Fe-BN/ZSM-5	CH_4 + CO + H_2O_2	30	101.8	66.0	1.90	[6]
			50	200.4	57.0	3.74	
8	Fe/ZSM-5	CH_4 + CO + H_2O_2	50	12000.0	63.2	537.76	[7]
9	Ni-ZSM-5	CH_4 + CO + H_2O_2	50	292.0	88.9	/	[8]
10	Pd_1/ZSM-5	CH_4 + CO + H_2O_2	25	968.0	78.2	/	[9]

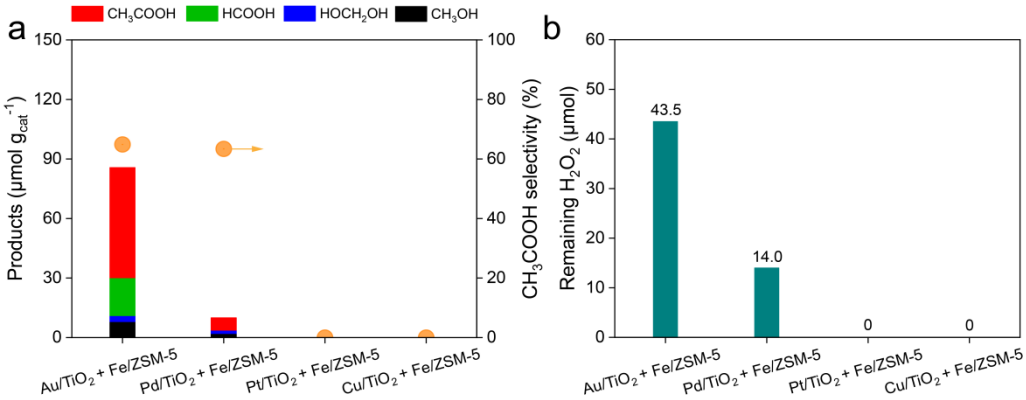

Figure S13. (**a**) Catalytic performance and (**b**) remaining H_2O_2 amount over M/TiO_2 (M= Au, Pd, Pt, Cu) and Fe/ZSM-5. The reaction was conducted over a total catalyst mass of 150 mg with mechanical stirring (1000 rpm) in 15 mL of H_2O under 15 bar of CH_4, 40 bar of CO, and 6 bar of O_2 at 30 °C for 6 h.

Table S8. CO partial pressure-dependent product yields over Au/TiO_2 + Fe/ZSM-5 under a standard condition except for CO partial pressure. The reaction was conducted over 150 mg of Au/TiO_2 + Fe/ZSM-5 with mechanical stirring (1000 rpm) in 15 mL of H_2O under 61 bar containing 15 bar of CH_4, 0~40 bar of CO, 6 bar of O_2, and N_2 as a balanced gas at 30 °C for 6 h.

CO Partial Pressure (bar)	Products (μmol g_{cat}^{-1})					CH_3COOH Selectivity (%)
	CH_3COOH	HCOOH	$HOCH_2OH$	CH_3OH	Total	
0	0	0	0	0	0	0
6	9.5	51.0	7.9	12.0	80.4	11.8
10	22.5	82.8	6.7	15.9	127.9	17.6
20	39.7	44.6	6.0	13.9	104.2	38.1
30	52.9	25.5	4.3	13.9	96.6	54.8
40	55.6	19.1	3.0	8.0	85.7	64.9

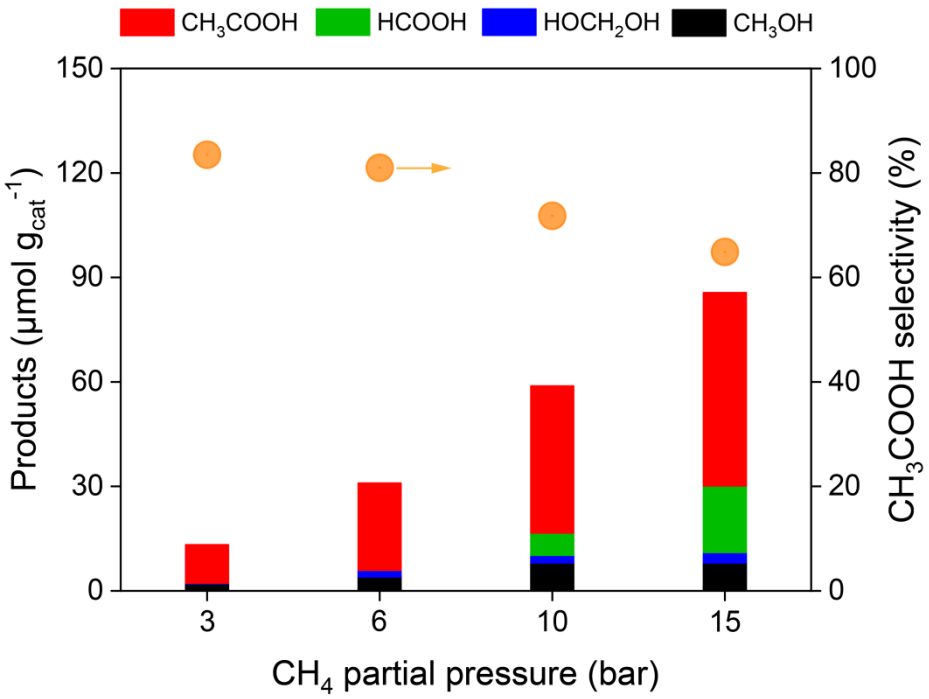

Figure S14. CH_4 partial pressure-dependent product yields over Au/TiO_2 + Fe/ZSM-5 under a standard condition except for CH_4 partial pressure. The reaction was conducted over 150 mg of Au/TiO_2 + Fe/ZSM-5 with mechanical stirring (1000 rpm) in 15 mL of H_2O under 61 bar containing 3~15 bar of CH_4, 40 bar of CO, 6 bar of O_2, and N_2 as a balanced gas at 30 °C for 6 h.

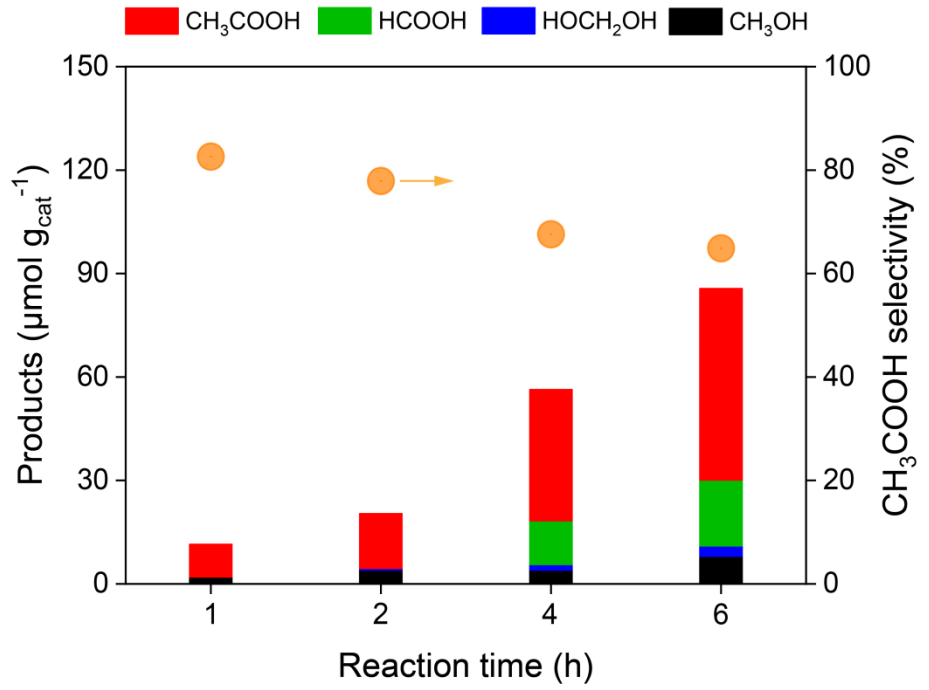

Figure S15. Time-dependent product yields over Au/TiO_2 + Fe/ZSM-5 under a standard condition except for the reaction time. The reaction was conducted over 150 mg of Au/TiO_2 + Fe/ZSM-5 with mechanical stirring (1000 rpm) in 15 mL of H_2O under 15 bar of CH_4, 40 bar of CO, and 6 bar of O_2 at 30 °C for 1~6 h.

Table S9. CH_4 partial pressure-dependent product yields over Au/TiO_2 + Fe/ZSM-5 under a standard condition except for CH_4 partial pressure. The reaction was conducted over 150 mg of Au/TiO_2 + Fe/ZSM-5 with mechanical stirring (1000 rpm) in 15 mL of H_2O under 61 bar containing 3~15 bar of CH_4, 40 bar of CO, 6 bar of O_2, and N_2 as a balanced gas at 30 °C for 6 h.

CH_4 Partial Pressure (bar)	Products (μmol g_{cat}^{-1})					CH_3COOH Selectivity (%)
	CH_3COOH	HCOOH	$HOCH_2OH$	CH_3OH	Total	
3	11.1	0	0.2	2.0	13.3	83.5
6	25.1	0	1.9	4.0	31.0	81.0
10	42.3	6.4	2.2	8.0	58.9	71.8
15	55.6	19.1	3.0	8.0	85.7	64.9

Table S10. Time-dependent product yields over Au/TiO_2 + Fe/ZSM-5 under a standard condition except for the reaction time. The reaction was conducted over 150 mg of Au/TiO_2 + Fe/ZSM-5 with mechanical stirring (1000 rpm) in 15 mL of H_2O under 15 bar of CH_4, 40 bar of CO, and 6 bar of O_2 at 30 °C for 1~6 h.

Reaction Time (h)	Products (μmol g_{cat}^{-1})					CH_3COOH in Liquid (%)
	CH_3COOH	HCOOH	$HOCH_2OH$	CH_3OH	Total	
1	9.5	0	0	2.0	11.5	82.6
2	15.9	0	0.5	4.0	20.4	77.9
4	38.1	12.7	1.6	4.0	56.4	67.6
6	55.6	19.1	3.0	8.0	85.7	64.9

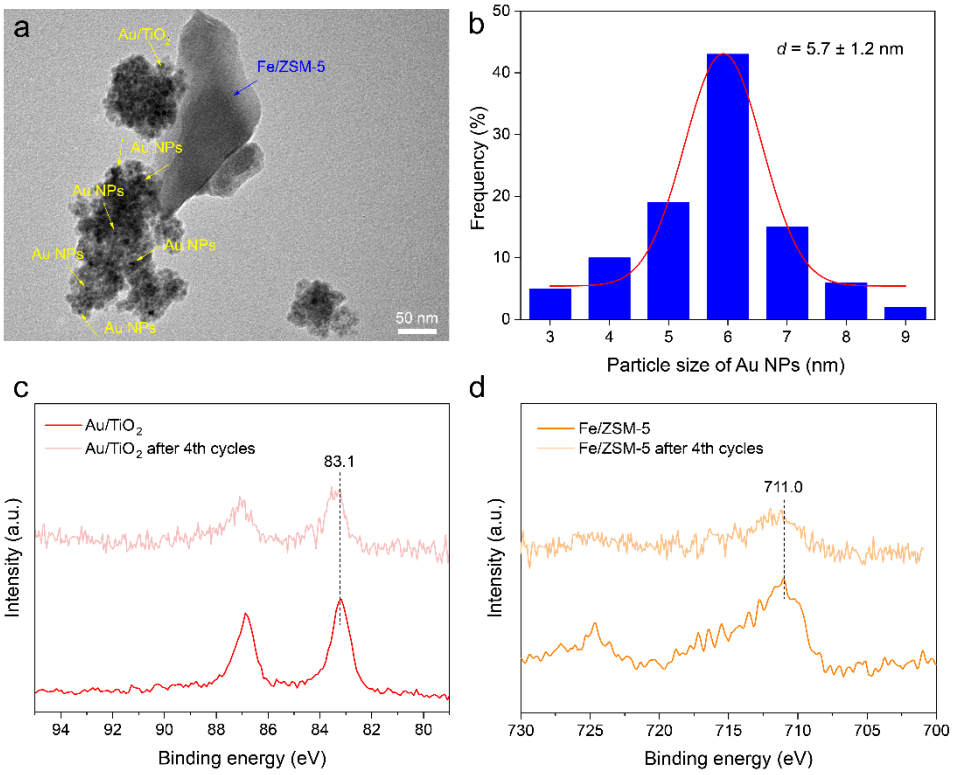

Figure S16. (**a**) TEM image and (**b**) Particle size distribution of Au nanoparticles for physically mixed Au/TiO_2 with Fe/ZSM-5 after fourth *in situ* cycles. (**c**) Au 4*f* XPS spectra for fresh and spent Au/TiO_2. (**d**) Fe 3*d* XPS spectra for fresh and spent Fe/ZSM-5.

Table S11. ICP-AES analysis after methane oxidation under standard reaction conditions.

Entry	Au in Catalyst (mg)	Au in Liquid (mg)	Fe in Catalyst (mg)	Fe in Liquid (mg)
1	0.26	0.00045	0.15	0.000075
2	0.51	0.00021	1	0.000045
3	0.85	0.00023	1	0.000015
4	1.36	0.00024	1	0.000015

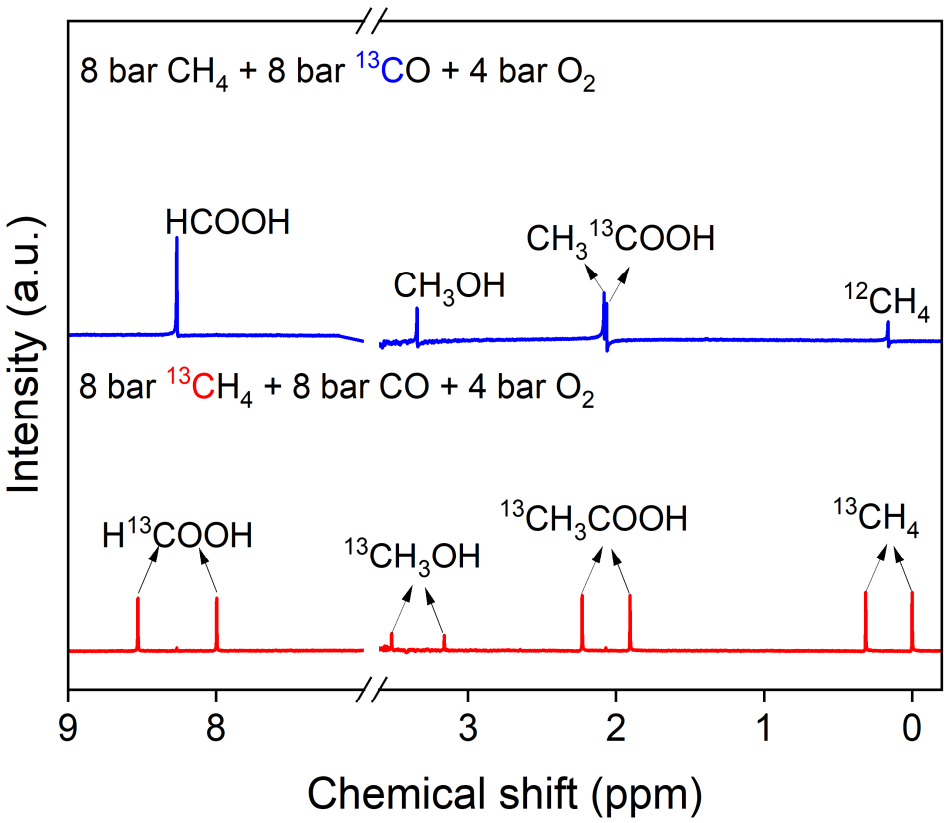

Figure S17. ^{1}H NMR spectrum for the isotopic labeling experiments. The reaction was conducted over 150 mg of Au/TiO_2 + Fe/ZSM-5 with mechanical stirring (1000 rpm) in 15 mL of H_2O under 8 bar of CH_4 (or 8 bar of $^{13}CH_4$), 8 bar of CO (or 8 bar of ^{13}CO), and 4 bar of O_2 at 30 °C for 6 h.

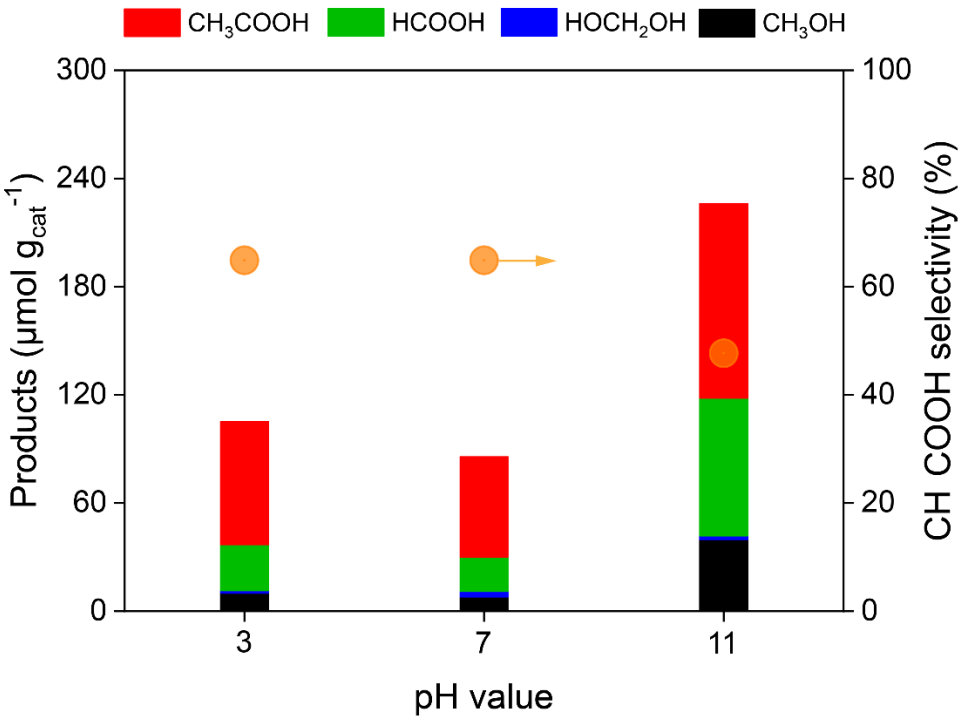

Figure S18. Effect of pH on catalytic performance under standard reaction conditions. HNO_3 and NaOH were used to adjust the pH value of the system.

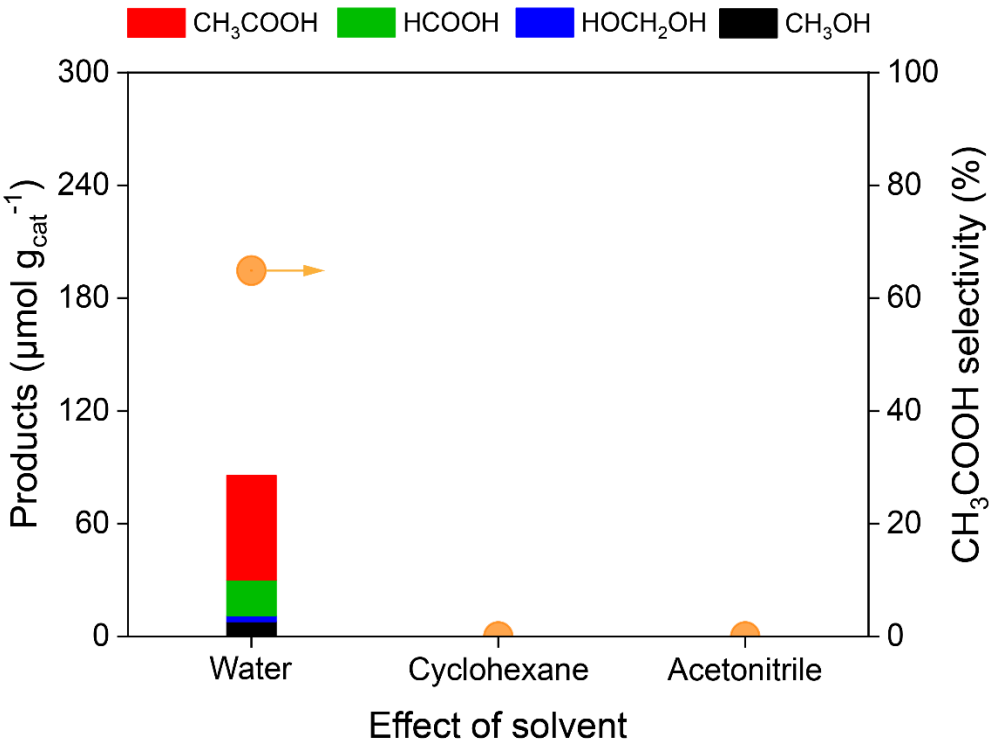

Figure S19. Effect of solvent on catalytic performance over 50 mg of Au/TiO_2 and 100 mg of Fe/ZSM-5 under standard reaction conditions.

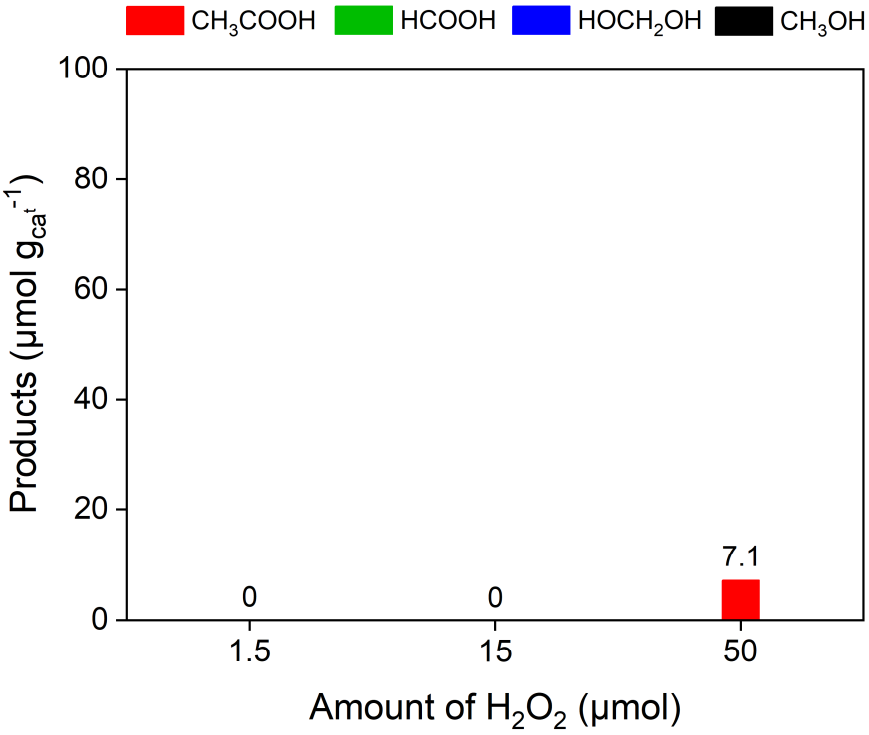

Figure S20. Methane oxidation with H_2O_2 in the presence of CO over Fe/ZSM-5. The reaction was conducted over 100 mg of Fe/ZSM-5 with mechanical stirring (1000 rpm) in 15 mL of H_2O containing 1.5~50 μmol of H_2O_2 under 15 bar of CH_4, 40 bar of CO, and 6 bar of N_2 at 30 °C for 1 h.

References

1. Gu, F.; Qin, X.; Pang, L.; Zhang, R.; Peng, M.; Xu, Y.; Hong, S.; Xie, J.; Wang, M.; Han, D.; et al. Acid-promoted selective oxidation of methane to formic acid over dispersed rhodium catalysts under mild conditions. *ACS Catal.* **2023**, *13*, 9509–9514.

2. Wu, B.; Yin, H.; Ma, X.; Liu, R.; He, B.; Li, H.; Zeng, J. Highly selective synthesis of acetic acid from hydroxyl-mediated oxidation of methane at low temperatures. *Angew. Chem. Int. Ed.* **2025**, *64*, e202412995.
3. Gu, F.; Qin, X.; Li, M.; Xu, Y.; Hong, S.; Ouyang, M.; Giannakakis, G.; Cao, S.; Peng, M.; Xie, J.; et al. Selective catalytic oxidation of methane to methanol in aqueous medium over copper cations promoted by atomically dispersed rhodium on TiO_2. *Angew. Chem. Int. Ed.* **2022**, *61*, e202201540.
4. Mao, J.; Liu, H.; Li, Y.; Gao, M.; Zhang, Y.; Song, Y.; Zhang, M.; Xu, G.; Zhou, W.; Yu, L.; et al. Mild-condition conversion of methane to acetic acid over MoS_2-confined Rh-Fe sites. *J. Am. Chem. Soc.* **2025**, *147*, 14530–14540.
5. Li, H.; Fei, M.; Troiano, J.; Ma, L.; Yan, X.; Tieu, P.; Yuan, Y.; Zhang, Y.; Liu, T.; Pan, X.; et al. Selective methane oxidation by heterogenized iridium catalysts. *J. Am. Chem. Soc.* **2023**, *145*, 769–773.
6. Wu, B.; Lin, T.; Lu, Z.; Yu, X.; Huang, M.; Yang, R.; Wang, C.; Tian, C.; Li, J.; Sun, Y.; et al. Fe binuclear sites convert methane to acetic acid with ultrahigh selectivity. *Chem* **2022**, *8*, 1658–1672.
7. Wang, C.; Sun, Y.; Wang, L.; Feng, W.; Miao, Y.; Yu, M.; Wang, Y.; Gao, X.; Zhao, Q.; Ding, Z.; et al. Oxidative carbonylation of methane to acetic acid on an Fe-modified ZSM-5 zeolite. *Appl Catal. B Environ.* **2023**, *329*, 122549.
8. Liu, J.; Wei, Y.; Li, R.; Liu, Y.; Yu, H.; Zhou, X.; Wu, B.; Lin, T.; Zhong, L. Isolated Ni sites anchored on zeolites for direct synthesis of acetic acid from methane oxidative carbonylation. *Appl. Catal. B Environ. Energy* **2024**, *350*, 123951.
9. Xu, W.; Liu, H.; Hu, Y.; Wang, Z.; Huang, Z.; Huang, C.; Lin, J.; Chang, C.; Wang, A.; Wang, X.; et al. Metal-oxo electronic tuning via in situ CO decoration for promoting methane conversion to oxygenates over single-atom catalysts. *Angew. Chem. Int. Ed.* **2024**, *136*, e202315343.